JOURNAL OF GEOPHYSICAL RESEARCH, VOL. 99, NO. D7, PAGES 14,565–14,573, JULY 20, 1994

Relationship of ozone and carbon monoxide over North America

Mian Chin, Daniel J. Jacob, and J. William Munger

Division of Applied Sciences and Department of Earth and Planetary Sciences, Harvard University, Cambridge, Massachusetts

David D. Parrish

NOAA Aeronomy Laboratory, Boulder, Colorado

Bruce G. Doddridge

Department of Meteorology, University of Maryland, College Park

Abstract. Observations at sites in eastern North America show a strong correlation between O_3 and CO concentrations in summer, with a consistent slope $\Delta O_3/\Delta CO \approx 0.3$. Observations in the aged Denver plume at Niwot Ridge, Colorado, also show a strong correlation but with $\Delta O_3/\Delta CO = 0.15$. These data offer a sensitive test for evaluating the ability of photochemical models to simulate production of O_3 over North America and its export to the global atmosphere. Application to the Harvard/Goddard Institute for Space Studies three-dimensional, continental-scale model shows that the model gives a good simulation of the observed O_3-CO correlations and of the associated $\Delta O_3/\Delta CO$. This successful simulation lends support to model estimates of 6 Gmol d^{-1} for the net O_3 production in the U.S. boundary layer in summer (corresponding to a net O_3 production efficiency of 5.5, which is the number of O_3 molecules produced per molecule of NO_x consumed) and 70% for the fraction of the net production that is exported to the global atmosphere. Export of U.S. pollution appears to make a significant contribution to total tropospheric O_3 over the northern hemisphere in summer. Simple interpretation of observed $\Delta O_3/\Delta CO$ as an O_3/CO anthropogenic enhancement ratio is shown to underestimate substantially anthropogenic O_3 production, because O_3 and CO concentrations are negatively correlated in the absence of photochemistry. It is also shown that concurrent observations of $\Delta O_3/\Delta CO$ and $\Delta O_3/\Delta(NO_y\text{-}NO_x)$ ratios can be used to impose lower and upper limits on the net O_3 production efficiency.

1. Introduction

Tropospheric O_3 is a key precursor of the hydroxyl radical which controls the oxidizing power of the atmosphere [*Logan et al.*, 1981; *Thompson*, 1992]. Ozone is also one of the major pollutants which, in high concentration, can be harmful to human health and to plants. Large amounts of anthropogenic O_3 are produced over the United States in summer by photochemical oxidation of nonmethane hydrocarbons (NMHCs) in the presence of nitrogen oxides ($NO_x = NO + NO_2$). Quantifying this anthropogenic source of O_3 and assessing its global influence is presently a major research issue in tropospheric chemistry [*Liu et al.*, 1987; *International Global Atmospheric Chemistry (IGAC)*, 1992; *Parrish et al.*, 1993].

The covariance of O_3 and CO concentrations offers a valuable constraint for quantifying the anthropogenic source of O_3. Carbon monoxide is a long-lived tracer of human activity with relatively well known sources from combustion, industry, and oxidation of hydrocarbons [*Logan et al.*, 1981]. Several authors have used the O_3-CO correlation measured from aircraft downwind of the United States to diagnose pollution influence on O_3 [*Fishman and Seiler*, 1983; *Fishman et al.*, 1987; *Chameides et al.*, 1987, 1989; *Marenco and Said*, 1989]. Recently, *Parrish et al.* [1993] made a first estimate of the export of anthropogenic O_3 from North America to the North Atlantic by using the slope $\Delta O_3/\Delta CO \approx 0.3$ measured at three Canadian marine sites downwind of the United States and scaling to a CO emission inventory for the eastern United States. They concluded that export of pollution from the United States dominates over transport from the stratosphere as a source of O_3 to the lower troposphere over the North Atlantic in summer.

A more detailed interpretation of $\Delta O_3/\Delta CO$ in terms of O_3 production requires a three-dimensional model that can resolve complicating factors such as the effect of O_3 deposition, the presence of chemical sources and sinks for CO, and spatial variability. We present here such an analysis using a continental-scale model for O_3 and its precursors over North America [*Jacob et al.*, 1993a]. Our principal objective is to use the O_3-CO correlation as a test of the ability of the model to compute production of O_3 over the continent. The particular value of this test is that it normalizes O_3 photochemical enhancements to a long-lived tracer of human activity. Ozone concentrations alone do not offer as sensitive a test because they include a substantial and variable background advected from the model boundaries (e.g., from the oceans or from high altitude). In rural surface

Paper number 94JD00907.
0148-0227/94/94JD-00907$05.00

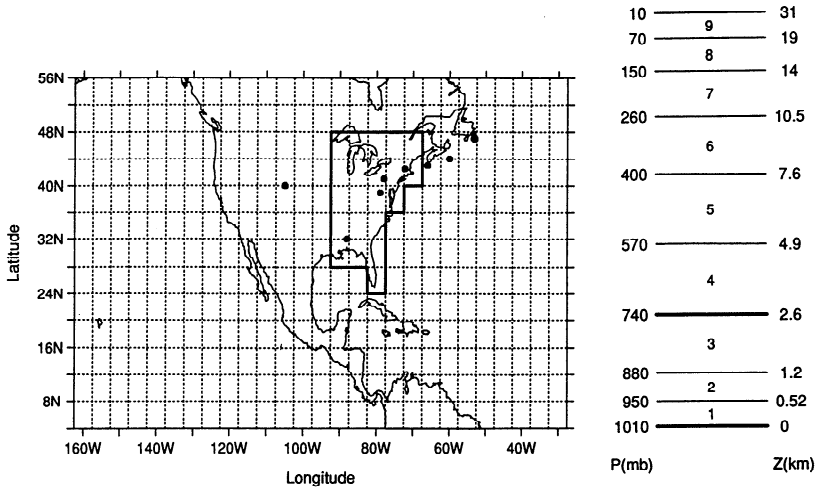

Figure 1. Model domain and grid. The vertical grid (nine layers) is defined by a sigma coordinate; pressures and altitudes at layer boundaries are shown for an atmospheric column based at sea level. Locations of the measurement sites are indicated by solid circles (see Table 1). The domain enclosed by thick lines and extending from the surface to 2.6 km altitude is the eastern U.S. boundary layer used in the text for budget calculations.

air over the eastern United States, about half of the mean summertime O_3 concentration appears to be contributed by advection from outside North America [*Jacob et al.*, 1993a]. The O_3-CO correlation removes to a large degree the sensitivity to background. As such, it diagnoses whether the model is giving a successful simulation of O_3 for the right reasons.

Section 2 gives a brief description of the model and summarizes important previous results. Section 3 presents observed O_3-CO correlations at sites in North America and compares model to observations. Section 4 assesses the possibility for direct interpretation of observed $\Delta O_3/\Delta CO$ as an anthropogenic enhancement ratio. Conclusions are in section 5.

2. The Model

The three-dimensional photochemical model of *Jacob et al.* [1993a] covers a domain including North and Central America and large portions of surrounding oceans with 4° latitude × 5° longitude grid resolution and nine vertical layers (Figure 1). Six tracers are transported, including odd oxygen (which is mainly O_3), CO, NO_x, peroxyacetylnitrates (PANs), and two lumped NMHCs. Anthropogenic emissions of NO_x, CO, and NMHCs in North America are taken from a summer 1985 inventory compiled by the National Acid Precipitation Assessment Program (NAPAP) [*Environmental Protection Agency (EPA)*, 1989]. Biogenic emission of isoprene and dry depositions of O_3, NO_x, and PANs, are computed using process models dependent on surface-type and meteorological variables. Chemical reaction rates are computed using the photochemical mechanism of *Lurmann et al.* [1986] with minor modifications [*Jacob et al.*, 1989]. Nonlinear chemistry in urban and industrial plumes is represented with a sub-grid-nested scheme in which concentrated pollution sources are forced to age in isolation for at least 8 hours before being mixed on the grid scale [*Sillman et al.*, 1990a].

The simulation is conducted for 3 summer months (June to August) with 2 weeks of initialization in May. Meteorological input is provided by one summer of data from a general circulation model (GCM) developed at the Goddard Institute of Space Studies (GISS) [*Hansen et al.*, 1983]. Meteorological variables are updated every 4 hours, and model output is also sampled every 4 hours. Boundary concentrations at the edges of Figure 1 are specified as a function of latitude, altitude, and month using observations.

The GCM is intended to simulate a typical year rather than any particular year; evaluation of model results with observations must therefore focus on seasonal statistics rather than on values for any particular day. *Jacob et al.* [1993a] previously evaluated the model with observed statistics for the concentrations of O_3 and precursors at rural sites in the United States. The model reproduces the observed summer median O_3 concentrations to within 5 ppb in most cases, except in the south central United States where concentrations are overpredicted by 15–20 ppb due in part to insufficient ventilation. Median summertime concentrations of CO are simulated to within 30 ppb at all sites, and the spatial variance of rural CO across the United States is well captured.

A detailed discussion of the O_3 budget in the three-dimensional model is given by *Jacob et al.* [1993b]. The net production rate of O_3 in the U.S. boundary layer (0–2.6 km altitude) averages 6.1 Gmol d^{-1} for the 3-month period June to August. The net O_3 production efficiency ε_N (net number of O_3 molecules produced per molecule of NO_x consumed, as defined by *Lin et al.* [1988]) has a mean value of 5.5 in the U.S. boundary layer and is more than 2 times higher in the western United States (9.1) than in the east (4.2) because of lower NO_x concentrations in the west. (Notice the slight changes of the values of O_3 production rate and net O_3 production efficiency from *Jacob et al.* [1993b], after correcting an error in saving those values.) Only 30% of the net O_3 production in the U.S. boundary layer in the model is deposited to the region; the remaining 70% is exported to the global atmosphere. This export amounts to about one fifth of

Table 1. O_3-CO Correlations at North American Sites in Summer

Site	Location	Period	n	Observation, Model: Median O_3, ppb	Median CO, ppb	$\Delta O_3/\Delta CO$, v/v	r^2	Reference
			Flatland					
Harvard Forest, Massachusetts	42°N, 72°W	June to Aug. 1990–1992	100	53	151	0.28 ± 0.02	0.78	J. Munger (unpublished data, 1993)
				51	149	0.29 ± 0.02	0.81	
Scotia, Pennsylvania	41°N, 78°W	July to Aug. 1988	96	73	212	0.28 ± 0.03	0.43	D. Parrish et al. (unpublished data, 1989)
				67	197	0.32 ± 0.02	0.84	
Kinterbish, Alabama	32°N, 88°W	June to July 1990	28	60	172	0.32 ± 0.05	0.57	D. Parrish et al. (unpublished data, 1991)
				64	159	0.41 ± 0.06	0.32	
			Mountaintop					
Shenandoah National Park, Virginia	39N, 79W, 1100 m	June to Aug. 1989	155	41	206	*a*	0.09	*Poulida et al.* [1991]
				63	176	0.31 ± 0.03	0.56	
Niwot Ridge, Colorado	40N, 105W, 3100 m	July to Aug. 1989	40	51	121	0.15 ± 0.02	0.50	D. Parrish et al. (unpublished data, 1990)
				65	131	0.18 ± 0.01	0.77	
			Marine					
Seal Island, Canada	43N, 66W	July to Aug. 1991	527	36	118	0.25 ± 0.01	0.77	*Parrish et al.* [1993][c]
				40	130	0.30 ± 0.01[b]	0.63	
Sable Island, Canada	44N, 60W	July to Aug. 1991	1098	36	107	0.30 ± 0.01	0.73	*Parrish et al.* [1993][c]
				38	123	0.31 ± 0.02[b]	0.59	
Cape Race, Canada	47N, 53W	July to Aug. 1991	1035	29	116	0.21 ± 0.01	0.47	*Parrish et al.* [1993][c]
				35	125	0.26 ± 0.02[b]	0.53	

Observation statistics are computed from hourly average data; for flatland and mountaintop sites, only data in the time window of 1300–1700 LT and with $NO_x/NO_y < 0.3$ are used (see text). Model statistics are computed from output sampled every 4 hours (model time step), in the 1300–1700 LT window for continental sites, and at all times of day at marine sites.

[a]Observed O_3 and CO concentrations are not correlated.

[b]Model correlations are computed for marine sites after removing points with O_3 less than 35 ppb and CO less than 120 ppb (background conditions), to focus on the pollution signal.

[c]September data reported by Parrish et al. are not included in the statistics.

the cross-tropopause transport of O_3 over the entire northern hemisphere in summer, implying that O_3 produced in the United States makes a significant contribution to tropospheric O_3 on the hemispheric scale.

3. O_3-CO Correlations

Table 1 summarizes observed and simulated O_3-CO correlation statistics for eight nonurban sites in North America where at least 1 month of observations are available in summer (June to August). Site locations are shown in Figure 1. For continental sites we restrict our attention to the 1300–1700 LT window, when surface air is most likely representative of the boundary layer. Such a restriction is not needed at marine sites where we use data for all times of day. The model gives one value per day in the 1300–1700 LT window at any site, the exact hour depending on longitude (1300 LT in Colorado, 1500 LT on the East Coast of the United States); we use that value for constructing model statistics. All statistics in the model are constructed for June to August ($n = 92$ points at continental sites; $n = 552$ points at marine sites), even when the observations cover only a fraction of that period.

Figure 2 plots observed O_3 versus CO concentrations at Harvard Forest in central Massachusetts. There is no significant correlation because of a number of points with elevated CO but low O_3, representing fresh pollution plumes that have not yet realized their O_3 production potential. Production of O_3 over the United States in summer is mostly NO_x limited [*Trainer et al.*, 1987; *Sillman et al.*, 1990b; *McKeen et al.*, 1991; *Chameides et al.*, 1992]; therefore realization of the O_3 production potential can be diagnosed by the NO_x/NO_y concentration ratio where NO_y represents the sum of NO_x and its oxidation products [*Trainer et al.*, 1993]. Figure 3 plots the NO_x/NO_y concentration ratio at Harvard Forest against the standard normal distribution. Two distinctly different populations are found: $NO_x/NO_y < 0.3$ (photochemically aged rural air) and $NO_x/NO_y > 0.3$ (fresh pollution). The rural air data (solid circles in Figure 2) show a strong correlation between O_3 and CO concentrations ($r^2 = 0.78$). This correlation is insensitive to small changes in the NO_x/NO_y criterion (using $NO_x/NO_y < 0.2$ as the criterion does not alter the correlation or the slope).

Figure 4 compares model results with rural observations (diagnosed by $NO_x/NO_y < 0.3$) at the five flatland and mountaintop sites listed in Table 1. The sites were chosen for the availability of concurrent observations for O_3, CO, NO_x, and NO_y. The measurements at Shenandoah include NO and NO_y concentrations but not NO_2 [*Doddridge et al.*, 1992]; we estimate the NO_2 concentrations at that site from $NO/NO_2/O_3$ photostationary steady state [*Leighton*, 1961], using local UV flux measurements to estimate the NO_2 photolysis rate constant [*Madronich*, 1987]. Selection of data with $NO_x/NO_y < 0.3$ is not possible in the model because NO_y is not a tracer; however, it is not necessary

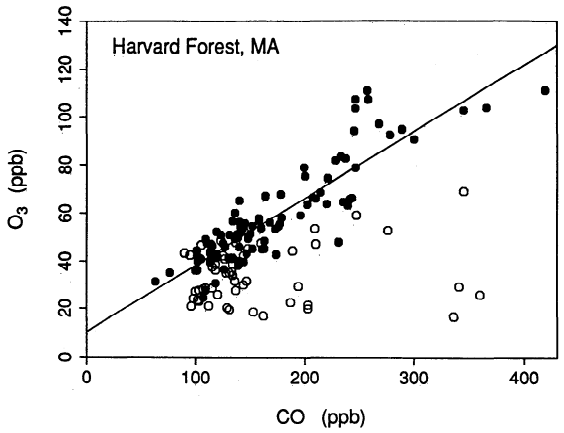

Figure 2. Hourly averaged O_3 and CO concentrations measured at Harvard Forest, Massachusetts, in June to August, 1300–1700 EST, 1990–1992. Solid and open circles represent hourly periods with a NO_x/NO_y concentration ratio less or greater than 0.3, respectively.

since urban and industrial pollution plumes are isolated in the model with the subgrid scheme.

The observations at Harvard Forest, Scotia (Pennsylvania), and Kinterbish (Alabama) show significant correlation between O_3 and CO concentrations, with $\Delta O_3/\Delta CO \approx 0.3$ at all three sites (Table 1). We find excellent agreement between model and observations at Harvard Forest for O_3 and CO concentrations and for the associated $\Delta O_3/\Delta CO$ (Figure 4a). The observations at Scotia are also well reproduced by the model, although the model has less scatter (Figure 4b). The model also reasonably agrees with the observations at Kinterbish; although the slope in the model is somewhat higher than in the observations (Figure 4c), they overlap within the standard error. The model does not, in general, capture the extremes in the observed concentrations, in part because of spatial averaging on the 4° × 5° grid scale.

Results for Shenandoah National Park, Virginia (mountaintop site, 1100 m altitude) are shown in Figure 4d. The observations show no significant O_3-CO correlation, while the model shows a strong correlation with slope $\Delta O_3/\Delta CO \approx 0.3$. The median concentration of O_3 in the model is 22 ppb higher than observed, while the median concentration of CO is 30 ppb lower. Model statistics are for the lowest layer (0–500 m altitude) to account for the upslope circulation in the daytime [*Poulida et al.*, 1991]; however, model results in layer 2 (corresponding to the actual altitude of the site) are not significantly different. The observations are from the summer of 1989, which was unusually cold, cloudy, and rainy; mean O_3 concentrations at the site that summer were 10 ppb lower than the average for the past six summers [*Poulida et al.*, 1991].

Results for Niwot Ridge, Colorado (3100 m) are shown in Figure 4e. The observations at Niwot Ridge sample, in general, either relatively clean air advected from the west or boundary layer air transported upslope from the east and contaminated by the Denver metropolitan area [*Parrish et al.*, 1990]. The O_3-CO correlation in the observations is driven by the Denver plume. We show in Figure 4e model results for air at the altitude of Niwot Ridge (open squares) and for the 4- to 8-hour-old Denver plume resolved with the subgrid scheme (open triangles). Model results seem consistent with observations. We find that $\Delta O_3/\Delta CO$ at Niwot Ridge is markedly lower than at rural eastern U.S. sites, both in the observations and in the model (Table 1). This result can be explained by the low NO_x/CO emission ratio in the Denver metropolitan area (0.14) as compared to the average for the eastern United States (0.23) [*EPA*, 1989]. The low NO_x/CO emission ratio in Denver reflects the dominance of mobile sources and fuel-rich combustion in automobiles not tuned to the local altitude of 1600 m [*Parrish et al.*, 1991].

Figure 5 compares model and observations at three Canadian marine sites [*Parrish et al.*, 1993]. These sites are downwind of the northeastern United States in the prevailing summertime circulation [*Wendland and Bryson*, 1981]. The observations indicate $\Delta O_3/\Delta CO$ in the range of 0.21 to 0.30, similar to values at eastern U.S. sites (Table 1). Model results are in good agreement. The variance in the model is far less than observed, certainly in part because aged pollution plumes are forced to dilute on the 4° × 5° grid scale (no cross-gridbox advection is allowed for subgrid plumes in the model).

Our analysis indicates that $\Delta O_3/\Delta CO \approx 0.3$ is a uniform characteristic of boundary layer air over eastern North America in summer. Data for the free troposphere from the Arctic Boundary Layer Expeditions (ABLE) 3A and 3B [*Harriss et al.*, 1992, 1994] are generally consistent with this result. *Wofsy et al.* [1992] measured $\Delta O_3/\Delta CO$ in the range 0.17–0.62 at 3–6 km altitude during an ABLE 3A flight along the eastern seaboard from Maine to Virginia. They measured a negative $\Delta O_3/\Delta CO$ below 1.5 km on the same flight, evidently due to O_3 deposition. Data from ABLE 3B show $\Delta O_3/\Delta CO$ in the range 0.20–0.69 for anthropogenic pollution plumes sampled in the free troposphere over eastern Canada [*Mauzerall et al.*, 1993].

4. Interpretation

We have shown that the three-dimensional model of *Jacob et al.* [1993a] reproduces closely the O_3-CO correlation and slope $\Delta O_3/\Delta CO$ for all available sites in North America except Shenandoah National Park. This finding, combined with the generally good simulation of O_3 and CO concentra-

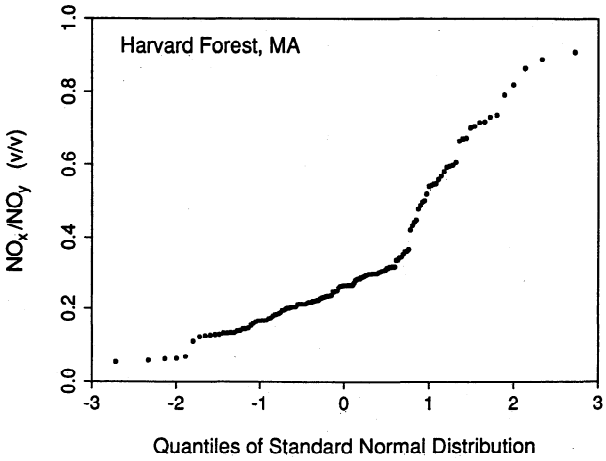

Figure 3. The NO_x/NO_y concentration ratio measured at Harvard Forest (for the same time period as in Figure 2) plotted against the standard normal distribution.

tions, lends confidence in the ability of the model to compute anthropogenic production of O_3 over the United States and the export of O_3 to the global atmosphere. Detailed discussion of model results, including O_3 budgets, is given by *Jacob et al.* [1993b].

We evaluate here the potential for a more direct interpretation of $\Delta O_3/\Delta CO$ as an O_3/CO anthropogenic enhancement ratio. *Parrish et al.* [1993] previously used this interpretation to estimate the export of O_3 from the United States to the North Atlantic. They multiplied the observed $\Delta O_3/\Delta CO \approx 0.3$ at the Canadian marine sites of Table 1 by a CO emission inventory for the United States east of Mississippi River (approximately east of 92°W) and inferred an export flux of 1.1 Gmol d^{-1} for anthropogenic O_3 out of the eastern United States (mostly, they assumed, to the North Atlantic). We find however in the model an export flux of 1.6 Gmol d^{-1} for anthropogenic O_3 out of the same region; this flux is 45% higher than estimated by *Parrish et al.* [1993], even though $\Delta O_3/\Delta CO$ in the model is indistinguishable from the observations. There are two principal reasons for the difference, as discussed below.

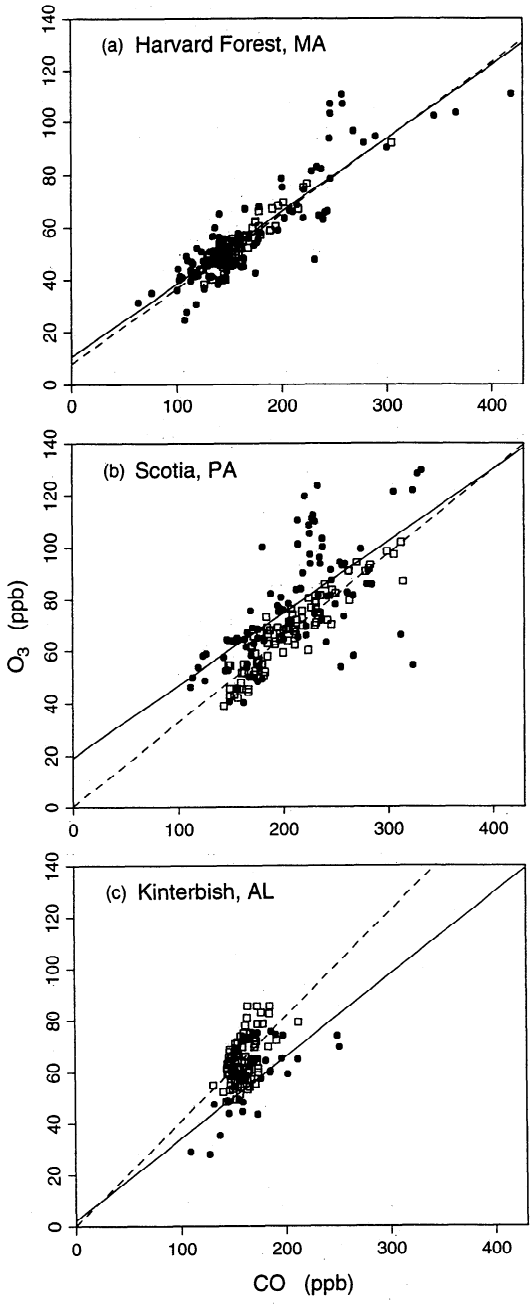

Figure 4. Observed and simulated O_3 and CO concentrations at five U.S. sites: (a) Harvard Forest, Massachusetts; (b) Scotia, Pennsylvania; (c) Kinterbish, Alabama; (d) Shenandoah National Park, Virginia; and (e) Niwot Ridge, Colorado. Details of the data are given in Table 1. Solid circles are observations and open squares are model values. In Figure 4e, model results are shown also for the aged Denver plume sampled with the sub-grid-nested scheme (open triangles). Lines are linear regressions to the observations (solid) and to the model results (dashed).

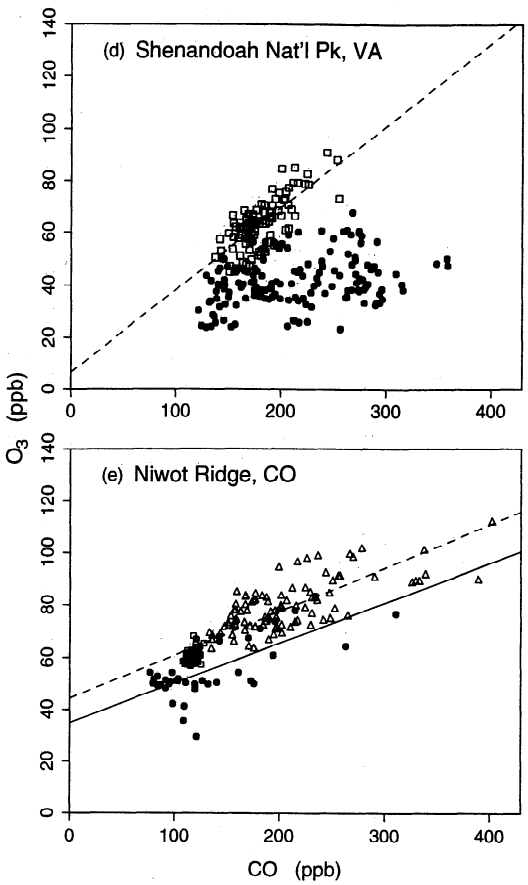

Figure 4. (continued)

First, the scaling of $\Delta O_3/\Delta CO$ as done by *Parrish et al.* [1993] could be improved by accounting for chemical sources and sinks of CO in addition to direct emission. Table 2 gives an inventory of CO sources and sinks for the continental boundary layer of the eastern United States in the three-dimensional model. Direct emission represents only 60% of the total CO source; the balance is contributed by atmospheric oxidation of hydrocarbons, in particular isoprene (20%). This chemical source is compensated by a strong chemical loss, reflecting the high concentrations of both CO and OH over the eastern United States. Overall, the net source of CO in the boundary layer of the eastern United States is 18% higher than the emission flux.

A more fundamental difficulty in interpreting observed $\Delta O_3/\Delta CO$ as an O_3/CO anthropogenic enhancement ratio is that in the absence of photochemistry, O_3 would be nega-

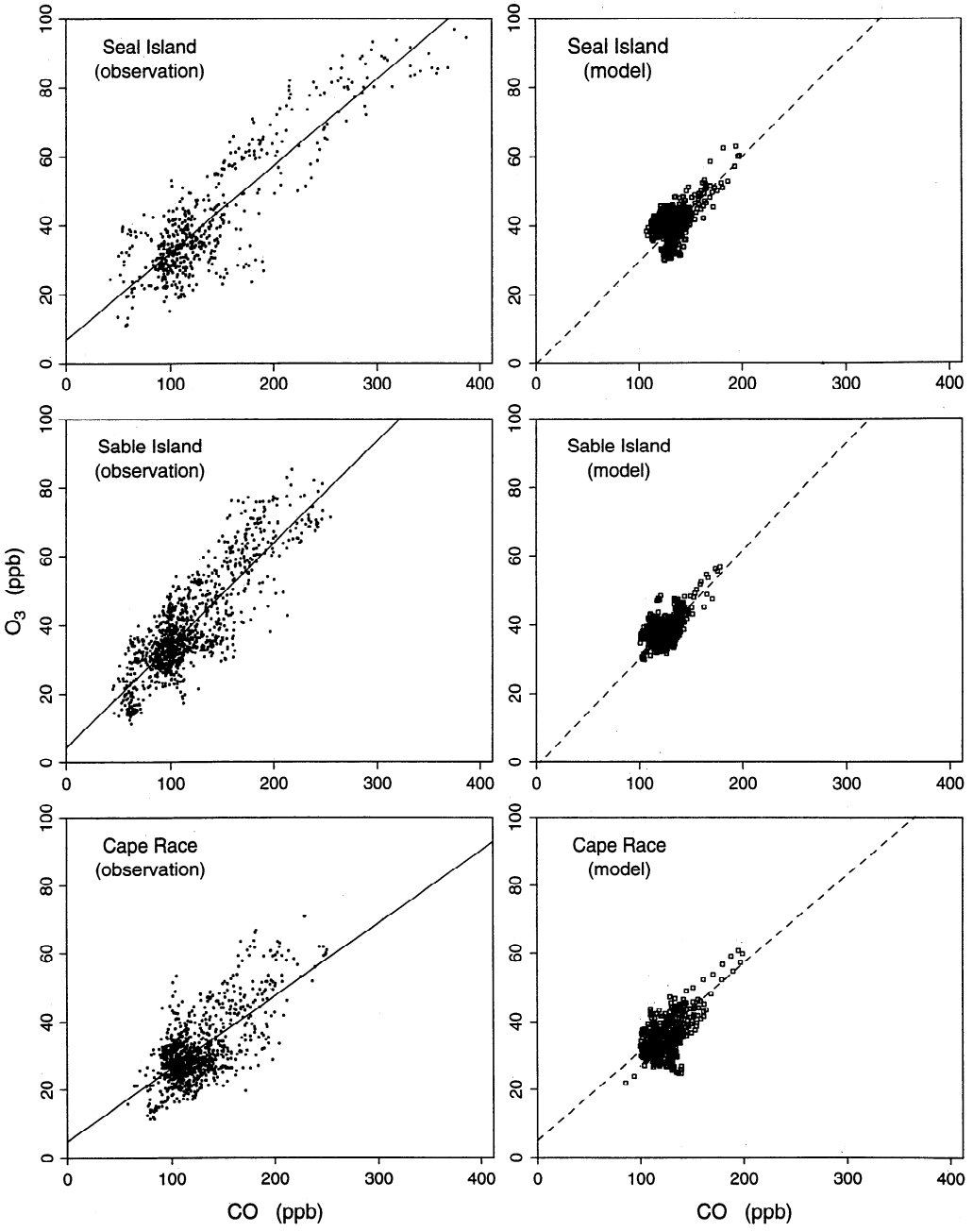

Figure 5. Observed and simulated O_3 and CO concentrations at three Canadian marine sites (Table 1). Lines are linear regressions.

tively correlated with CO due to deposition. As a result, the measured $\Delta O_3/\Delta CO$ is less than the actual anthropogenic enhancement ratio. We determined the magnitude of this effect by conducting a model simulation with O_3 concentrations regulated solely by advection of boundary conditions and deposition (no chemical production or loss). Figure 6 shows the results for Seal Island, Canada; without photochemistry, O_3 and CO concentrations are negatively correlated (crosses, top panel). We can define an O_3 photochemical enhancement as the difference between the O_3 concentrations in the standard simulation and those in the simulation including no chemistry. This photochemical enhancement of O_3 shows a strong positive correlation with CO (solid squares, bottom panel). The slope in the bottom panel (0.40) gives the actual O_3/CO enhancement ratio from U.S. pollution; it is 33% higher than $\Delta O_3/\Delta CO$ in the top panel (0.30).

We now turn to the application of $\Delta O_3/\Delta CO$ as a measure of the O_3 production efficiency. *Liu et al.* [1987] pointed out that the O_3 production is best referenced to the loss of NO_x or, on a regional scale, the emission of NO_x, since O_3 production is NO_x limited. A net O_3 production efficiency ε_N was defined by *Lin et al.* [1988] as the net number of O_3 molecules produced per NO_x molecule consumed. By scaling the observed $\Delta O_3/\Delta CO$ in photochemically aged air to a CO/NO_x source ratio, we can obtain an estimate of the net O_3 production efficiency ε_N; such an estimate is however a lower limit because of deposition of O_3. The CO/NO_x source

ratio for the eastern United States, as defined in Figure 1, is 5.6 (using the net CO source in Table 2 and the NAPAP emission inventory for NO_x). From $\Delta O_3/\Delta CO = 0.3$, we obtain a net O_3 production efficiency ε_N of 1.7 in eastern U.S. boundary layer. In comparison a value of 8.5 for ε_N at Scotia and at Egbert, Ontario, was estimated by *Trainer et al.* [1993] using observations of $\Delta O_3/\Delta(NO_y\text{-}NO_x)$, and *Olszyna et al.* [1993] found a ε_N value of 12 at Tennessee using the same relationship; these values would be upper limits for ε_N because of rapid HNO_3 deposition. Our three-dimensional model gives a mean value $\varepsilon_N = 4.2$ for the eastern United States [*Jacob et al.*, 1993b], which is intermediate between the lower and the upper limits imposed by the observations of $\Delta O_3/\Delta CO$ and $\Delta O_3/\Delta(NO_y\text{-}NO_x)$.

We have seen that deposition of O_3 is an important factor limiting the potential for simple interpretation of the O_3-CO correlation in terms of O_3 production. Model results indicate that this effect is greatest in the central United States, where O_3 concentrations would be at a minimum in the absence of photochemistry because of the long fetch in the continental boundary layer [*Jacob et al.*, 1993a]. Figure 7 shows O_3-CO correlations for the Oregon, Nebraska, Illinois, and Massachusetts grid boxes; there is no significant correlation between O_3 and CO in the Nebraska grid box. By subtracting the O_3 concentration computed in the absence of photochemistry (as in Figure 6), we obtain a strong correlation between O_3 photochemical enhancement and CO (solid squares in Figure 7). The slope of the linear regression analysis of the O_3 photochemical enhancement versus CO falls within a narrow range (0.33 to 0.49) for the four grid boxes in Figure 7 and is actually highest in the Nebraska grid box.

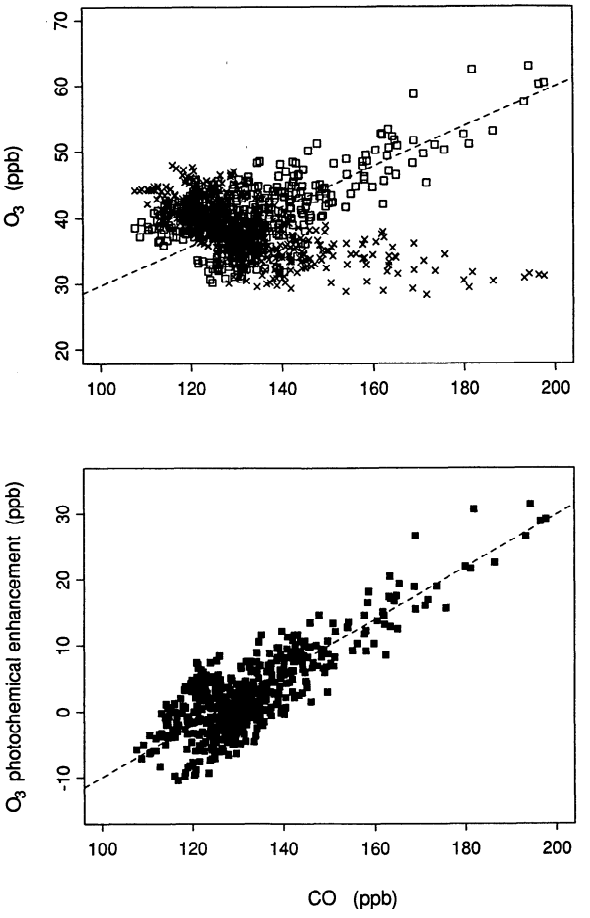

Figure 6. Simulated O_3 and CO concentrations at Seal Island, Canada, in the model. The top panel shows O_3 in the standard simulation (open squares) and in a simulation with no photochemistry (crosses); the bottom panel shows the O_3 photochemical enhancement defined as the difference. The lines are linear regressions to standard O_3 and CO (top panel) and to O_3 photochemical enhancement and CO (bottom panel).

5. Conclusion

Observations at nonurban sites in eastern North America show a strong correlation between O_3 and CO concentrations in photochemically aged air (as defined by $NO_x/NO_y < 0.3$). The slope, $\Delta O_3/\Delta CO$, has a remarkably uniform value of about 0.3. Observations at Niwot Ridge, Colorado, indicate $\Delta O_3/\Delta CO = 0.15$ in the aged Denver plume; this low value is attributed to the low NO_x/CO emission ratio in the Denver metropolitan area.

The O_3-CO relationship provides a sensitive test of O_3 production in chemical transport models. We used it to test a three-dimensional, continental-scale model of O_3 and precursors over North America [*Jacob et al.*, 1993a]. The model captures successfully the O_3-CO correlations and reproduces closely the observed $\Delta O_3/\Delta CO$. It does not capture the full extent of variance in the observations, certainly in part because of spatial averaging on the grid scale. Simulation of the O_3-CO relationship lends confidence in the ability of the model to compute photochemical production of O_3 over North America and its export to the global atmosphere [*Jacob et al.*, 1993b].

We investigated the possibility for a more direct interpretation of observed $\Delta O_3/\Delta CO$ as an O_3/CO anthropogenic enhancement ratio, to be multiplied by a CO source estimate for quantitative inference of photochemical O_3 production and export. A first complication with this simple approach is the need to account for chemical sources and sinks of CO, even in a highly polluted region such as the eastern United States. A second complication is that O_3 concentrations over polluted regions include a major component advected from outside the region, which is negatively correlated with CO due to deposition at the surface. As a result, $\Delta O_3/\Delta CO$ measured at sites over the United States and downwind is

Table 2. Budget of CO for the Boundary Layer of the Eastern United States

	Rate, Gmol d^{-1}
Sources	
Anthropogenic emission	3.3
Oxidation of isoprene	1.1
Oxidation of anthropogenic NMHCs	0.5
Oxidation of CH_4	0.6
Sink	
Reaction with OH	−1.6
Net CO source	3.9

This budget is based on model results from June to August for the region enclosed by thick lines in Figure 1. Anthropogenic emission is from the National Acid Precipitation Assessment Program inventory. NMHCs, nonmethane hydrocarbons.

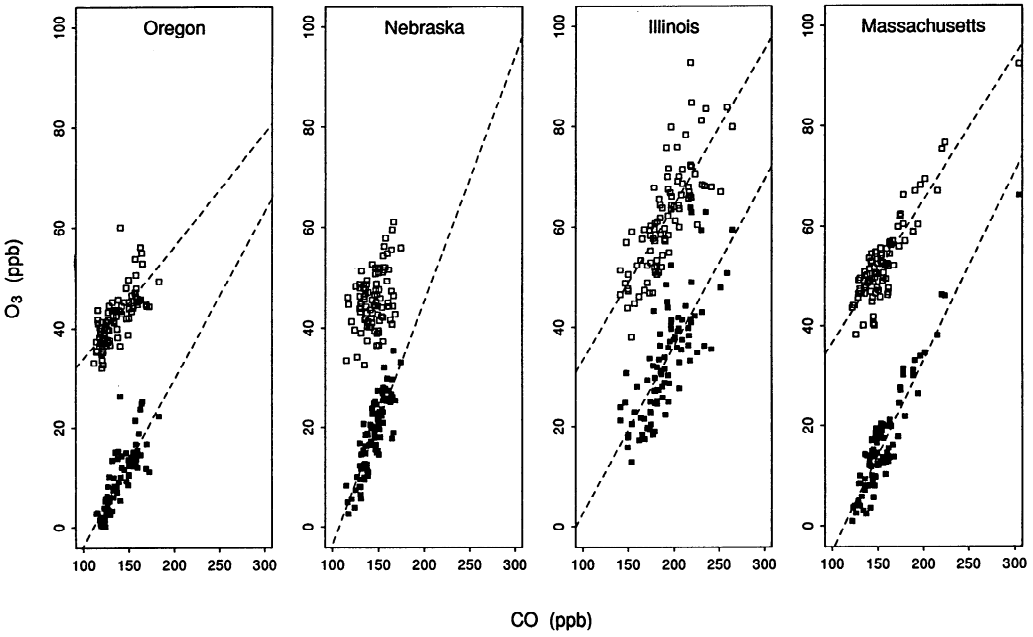

Figure 7. Simulated O_3 and CO concentrations in June to August (1200–1500 LT) for the Oregon, Nebraska, Illinois, and Massachusetts surface grid boxes. The open squares show O_3 concentrations from the standard simulation; the solid squares show the O_3 photochemical enhancement. The slopes and correlations for standard O_3 versus CO are Oregon, slope = 0.22, r^2 = 0.53; Nebraska, no significant correlation (r^2 = 0.15); Illinois, slope = 0.31, r^2 = 0.61; and Massachusetts, slope = 0.29, r^2 = 0.81. The slopes and correlations for the O_3 photochemical enhancement versus CO are Oregon, slope = 0.39, r^2 = 0.74; Nebraska, slope = 0.49, r^2 = 0.74; Illinois, slope = 0.33, r^2 = 0.60; and Massachusetts, slope = 0.39, r^2 = 0.87.

significantly less than the O_3/CO anthropogenic enhancement ratio, and the direct interpretation of observed $\Delta O_3/\Delta CO$ may underestimate substantially the O_3 production and export.

From the $\Delta O_3/\Delta CO$ observed in the eastern United States scaled to a CO/NO_x source ratio for the region, we infer a lower limit of 1.7 for the net O_3 production efficiency ε_N defined as the net number of O_3 molecules produced per molecule of NO_x consumed. This value is a lower limit because of O_3 deposition. Observations of $\Delta O_3/\Delta(NO_y\text{-}NO_x)$ in the eastern United States yield values of 8.5–12 for ε_N; these values are upper limit because of rapid HNO_3 deposition. The mean ε_N value of 4.2 computed in the three-dimensional model for the boundary layer of the eastern United States falls within the limits imposed by the observations of $\Delta O_3/\Delta CO$ and $\Delta O_3/\Delta(NO_y\text{-}NO_x)$.

Acknowledgments. We thank Steve Wofsy and Jennifer Logan for their comments and suggestions. This work was supported by grants to Harvard University (National Science Foundation, NSF-93-04217 and NSF-BSR-8919300; the National Aeronautics and Space Administration, NASA-NAGW-3082; Environmental Protection Agency, EPA-R814535-01-0; Department of Energy, Northeastern Center of the Global Environmental Change; and the Packard Foundation), grants to the University of Maryland (Environmental Protection Agency, EPA-R814526 and National Science Foundation, ATM-86-19491 and ATM-90-14841), and part of the Climate and Global Change Program by the National Oceanic and Atmospheric Administration.

References

Chameides, W. L., D. D. Davis, M. O. Rodgers, J. Bradshaw, S. Sandholm, G. Sachse, G. Hill, G. Gregory, and R. Rasmussen, Net ozone photochemical production over the eastern and central north Pacific as inferred from CTE/CITE 1 observations during fall 1983, *J. Geophys. Res.*, *92*, 2131–2152, 1987.

Chameides, W. L., D. D. Davis, G. L. Gregory, G. Sachse, and A. L. Torres, Ozone precursors and ozone photochemistry over eastern North Pacific during the spring of 1984 based on the NASA GTE/CITE 1 airborne observations, *J. Geophys. Res.*, *94*, 9799–9808, 1989.

Chameides, W. L., et al., Ozone precursor relationships in the ambient atmosphere, *J. Geophys. Res.*, *97*, 6037–6055, 1992.

Doddridge, B. G., R. R. Dickerson, R. G. Wardell, K. L. Civerolo, and L. J. Nunnermacker, Trace gas concentrations and meteorology in rural Virginia, 2, Reactive nitrogen compounds, *J. Geophys. Res.*, *97*, 20,631–20,646, 1992.

Environmental Protection Agency (EPA), The 1985 NAPAP emission inventory (version 2): Development of the annual data and modeler's tapes, *Rep. EPA-600/7-89-012a*, Environ. Prot. Agency, Research Triangle Park, N. C., 1989.

Fishman, J., and W. Seiler, Correlative nature of ozone and carbon monoxide in the troposphere: Implications for the tropospheric ozone budget, *J. Geophys. Res.*, *88*, 3662–3670, 1983.

Fishman, J., G. L. Gregory, G. W. Sachse, S. M. Beck, and G. F. Hill, Vertical profiles of ozone, carbon monoxide, and dew point temperature obtained during GTE/CITE 1, October to November 1983, *J. Geophys. Res.*, *92*, 2083–2094, 1987.

Hansen, J., G. Russell, D. Rind, P. Stone, A. Lacis, S. Lebedeff, R. Ruedy, and L. Travis, Efficient three-dimensional global models for climate studies: Models I and II, *Mon. Weather Rev.*, *111*, 609–662, 1983.

Harriss, R. C., et al., The Arctic Boundary Layer Expedition (ABLE 3A): July to August 1988, *J. Geophys. Res.*, *97*, 16,383–16,394, 1992.

Harriss, R. C., et al., The Arctic Boundary Layer Expedition (ABLE 3B): July to August 1990, *J. Geophys. Res.*, *99*, 1635–1643, 1994.

International Global Atmospheric Chemistry (IGAC), Core Project Office, *International Global Atmospheric Chemistry (IGAC) Project: An Overview*, MIT Press, Cambridge, Mass., 1992.

Jacob, D. J., S. Sillman, J. A. Logan, and S. C. Wofsy, Least independent variables method for simulation of tropospheric ozone, *J. Geophys. Res.*, *94*, 8497–8509, 1989.

Jacob, D. J., et al., Simulation of summertime ozone over North America, *J. Geophys. Res.*, *98*, 14,797–14,816, 1993a.

Jacob, D. J., J. A. Logan, G. M. Gardner, R. M. Yevich, C. M. Spivakovsky, S. C. Wofsy, S. Sillman, and M. J. Prather, Factors regulating ozone over the United States and its export to the global atmosphere, *J. Geophys. Res.*, *98*, 14,817–14,826, 1993b.

Leighton, P. A., *Photochemistry of Air Pollution*, Academic, San Diego, Calif., 1961.

Lin, X., M. Trainer, and S. C. Liu, On the nonlinearity of the tropospheric ozone production, *J. Geophys. Res.*, *93*, 15,879–15,888, 1988.

Liu, S. C., M. Trainer, F. C. Fehsenfeld, D. D. Parrish, E. J. Williams, E. W. Fahey, G. Hubler, and P. C. Murphy, Ozone production in the rural troposphere and the implications for regional and global ozone distribution, *J. Geophys. Res.*, *92*, 4191–4207, 1987.

Logan, J. A., M. J. Prather, S. C. Wofsy, and M. B. McElroy, Tropospheric chemistry: A global perspective, *J. Geophys. Res.*, *86*, 7210–7254, 1981.

Lurmann, F. W., A. C. Lloyd, and R. Atkinson, A chemical mechanism for use in long-range transport/acid deposition computer modeling, *J. Geophys. Res.*, *91*, 10,905–10,936, 1986.

Madronich, S., Intercomparison of NO_2 photodissociation and u.v. radiometer measurements, *Atmos. Environ.*, *21*, 569–578, 1987.

Marenco, A., and F. Said, Meridional and vertical ozone distribution in the background troposphere (70°N–60°S; 0–12 km altitude) from scientific aircraft measurements during the STRATOZ III experiment (June 1984), *Atmos. Environ.*, *23*, 201–214, 1989.

Mauzerall, D. L., D. J. Jacob, S.-M. Fan, J. D. Bradshaw, S. T. Sandholm, D. R. Blake, G. L. Gregory, and G. W. Sachse, An ozone budget for the remote troposphere over eastern Canada, *Eos Trans. AGU*, *74*, Fall Meeting suppl., *74*(43), 180, 1993.

McKeen, S. A., E.-Y. Hsie, M. Trainer, R. Tallamraju, and S. C. Liu, A regional model study of the ozone budget in the eastern United States, *J. Geophys. Res.*, *96*, 10,809–10,845, 1991.

Olszyna, K. J., E. M. Bailey, and J. F. Meagher, O_3 and NO_y relationships at a rural site in Tennessee, *Eos Trans. AGU*, *74*, Spring Meeting suppl., *74*(16), 66, 1993.

Parrish, D. D., et al., Systematic variations in the concentration of NO_x (NO plus NO_2) at Niwot Ridge, Colorado, *J. Geophys. Res.*, *95*, 1817–1836, 1990.

Parrish, D. D., M. Trainer, M. P. Buhr, B. A. Watkins, and F. C. Fehsenfeld, Carbon monoxide concentrations and their relation to concentrations of total reactive oxidized nitrogen at two rural U.S. sites, *J. Geophys. Res.*, *96*, 9309–9320, 1991.

Parrish, D. D., J. S. Holloway, M. Trainer, P. C. Murphy, G. L. Forbes, and F. C. Fehsenfeld, Export of North American ozone pollution to the North Atlantic Ocean, *Science*, *259*, 1436–1439, 1993.

Poulida, O., R. R. Dickerson, B. G. Doddridge, J. Z. Holland, R. G. Wardell, and J. G. Watkins, Trace gas concentrations and meteorology in rural Virginia, 1, Ozone and carbon monoxide, *J. Geophys. Res.*, *96*, 22,461–22,475, 1991.

Sillman, S., J. A. Logan, and S. C. Wofsy, A regional scale model for ozone in the United States with subgrid representation of urban and power plant plumes, *J. Geophys. Res.*, *95*, 5731–5748, 1990a.

Sillman, S., J. A. Logan, and S. C. Wofsy, The sensitivity of ozone to nitrogen oxides and hydrocarbons in regional ozone episodes, *J. Geophys. Res.*, *95*, 1837–1851, 1990b.

Thompson, A. M., The oxidizing capacity of the Earth's atmosphere: Probable past and future changes, *Science*, *256*, 1157–1168, 1992.

Trainer, M., E. Y. Hsie, S. A. McKeen, R. Tallamraju, D. D. Parrish, F. C. Fehsenfeld, and S. C. Liu, Impact of natural hydrocarbons on hydroxyl and peroxy radicals at a remote site, *J. Geophys. Res.*, *92*, 11,879–11,894, 1987.

Trainer, M., et al., Correlation of ozone with NO_y in photochemically aged air, *J. Geophys. Res.*, *98*, 2917–2925, 1993.

Wendland, W. M., and R. A. Bryson, Northern hemisphere airstream regions, *Mon. Weath. Rev.*, *109*, 255–270, 1981.

Wofsy, S. C., et al., Atmospheric chemistry in the Arctic and subarctic: Influence of natural fires, industrial emissions, and stratospheric inputs, *J. Geophys. Res.*, *97*, 16,731–16,746, 1992.

M. Chin, D. J. Jacob, and W. Munger, Division of Applied Sciences and Department of Earth and Planetary Sciences, Harvard University, Cambridge, MA 02138.

B. G. Doddridge, Department of Meteorology, University of Maryland, College Park, MD 20742.

D. D. Parrish, NOAA Aeronomy Laboratory, Boulder, CO 80303.

(Received November 23, 1993; revised March 25, 1994; accepted April 1, 1994.)